Journal of Biomechanical Engineering. Received January 02, 2020;
Accepted manuscript posted April 15, 2020. doi:10.1115/1.4046921

A Method to Quantify Tensile Biaxial Properties of Mouse Aortic Valve Leaflets

Daniel Chaparro[1]*, Valentina Dargam[1]*, Paulina Alvarez[1], Jay Yeung[1], Ilyas Saytashev[1], Jenniffer Bustillo[2], Archana Loganathan[2], Jessica Ramella-Roman[1], Arvind Agarwal[2], Joshua D. Hutcheson[1,3]

[1] Department of Biomedical Engineering, Florida International University, Miami, FL, 33174, USA

[2] Department of Mechanical and Materials Engineering, Florida International University, Miami, FL, 33174, USA

[3] Biomolecular Sciences Institute, Florida International University, Miami, FL, 33199, USA

*** These authors contributed equally**

Correspondence:

Dr. Joshua D. Hutcheson
Department of Biomedical Engineering
Florida International University
Phone: 305-348-0157
Fax: 305-348-6954
Email: jhutches@fiu.edu

Key Words: mouse aortic valve mechanics, aortic valve, anisotropy.

Journal of Biomechanical Engineering. Received January 02, 2020;
Accepted manuscript posted April 15, 2020. doi:10.1115/1.4046921

ABSTRACT

Understanding aortic valve (AV) mechanics is crucial in elucidating both the mechanisms that drive the manifestation of valvular diseases as well as the development of treatment modalities that target these processes. Genetically modified mouse models have become the gold standard in assessing biological mechanistic influences of AV development and disease. However, very little is known about mouse aortic valve leaflet (MAVL) tensile properties due to their microscopic size (~500μm long and 45μm thick) and the lack of proper mechanical testing modalities to assess uniaxial and biaxial tensile properties of the tissue. We developed a method in which the biaxial tensile properties of MAVL tissues can be assessed by adhering the tissues to a silicone rubber membrane utilizing dopamine as an adhesive. Applying equiaxial tensile loads on the tissue-membrane composite and tracking the engineering strains on the surface of the tissue resulted in the characteristic orthotropic response of AV tissues seen in human and porcine tissues. Our data suggests that the circumferential direction is stiffer than the radial direction (n=6, P=0.0006) in MAVL tissues. This method can be implemented in future studies involving longitudinal mechanical stimulation of genetically modified MAVL tissues bridging the gap between cellular biological mechanisms and valve mechanics in popular mouse models of valve disease.

INTRODUCTION

Understanding aortic valve (AV) mechanics is crucial in elucidating both the mechanisms that drive the manifestation of valvular diseases as well as the development of treatment modalities that target these processes. Orthogonally aligned elastin and collagen fibers dictate AV structure and function [1]. Radially aligned elastin fibers allow the AV leaflets to stretch toward the center of the AV orifice during diastole, preventing retrograde blood flow. Circumferentially aligned collagen fibers provide the necessary tensile strength to prevent leaflet prolapse under this diastolic load. Alterations in fiber structure and composition within the AV compromise valve mechanics and thus function [2]. AV leaflet mechanics have traditionally been quantified using uniaxial or biaxial tensile testing modalities in which the tensile stiffness of these tissues in the radial and circumferential directions can be determine [3-5]. Studies including these tests have extensively reported the characteristic orthotropic response of AV leaflets in which the radial direction is softer than the circumferential direction.

Genetically modified mouse models recapitulating certain aspects of human AVs have facilitated mechanistic studies of AV development, congenital defects, and disease progression [6]. However, as convenient as these mouse models are in clarifying some of the biological mechanisms behind AV development and disease progression, very little is known about the gross mechanical properties of the mouse AV due to its microscopic size (~500μm long and 45μm thick) [7]. As such, traditional uniaxial and biaxial tensile testers cannot be implemented to mouse aortic valve leaflet (MAVL) tissues.

Biomechanical analyses of MAVLs have traditionally employed local strain measurement techniques such as atomic force microscopy, nanoindentation, and micropipette aspiration [8-10]. While these techniques may be used to quantify regional differences in MAVL tissue stiffness, they displace MAVL tissues perpendicular to the radial/circumferential plane. Therefore, these techniques do not recreate the physiologically relevant loads and displacements experienced by AV leaflets *in vivo* and are also unable to determine anisotropic tensile properties of the tissue. Physiologically-relevant mechanical testing of MAVL tissues that recapitulate biaxial tests performed in human and porcine valves are needed to better understand the relationship between human and mouse AVs and connect the biomolecular insight provided by mouse models to AV biomechanics [11].

In this study we developed a method to determine MAVL anisotropic tensile properties by adhering the tissue to a silicone membrane coated with dopamine. A Flexcell system was used to induce equiaxial tensile loads on the tissue-

membrane composite, and a custom MATLAB script was used to determine the engineering strains in the radial and circumferential directions on the leaflet surface. We demonstrate anisotropic MAVL behavior that mimics previous observations from human and porcine AV tensile testing.

METHODOLOGY

Dopamine Coating and Tissue Preparation

StageFlexer (Flexcell International, Burlington, North Carolina) membranes were treated with dopamine (A11136 Dopamine Hydrochloride 99%, Alfa Aesar) (0.1, 0.3, 0.5 mg/mL) in 0.01M Tris buffer solution and left at room temperature overnight (~18 hours). Polydopamine has been shown to promote adhesion of biological samples to synthetic surfaces [12, 13]. Polydopamine coated surfaces have shown to reduce substrate surface hydrophobicity and promote in-vitro tissue development [14]. Therefore, dopamine solutions were used to promote adhesion between substrate surface and tissue.

C57/BL6 wild type mouse hearts were transported to the laboratory in ice cold 1xPBS where a stereoscopic zoom microscope (Nikon SMZ645) was used to dissect the hearts and resect the AV leaflets (**Fig. 1**). Tissues were periodically rinsed with ice cold 1xPBS to prevent drying. A transverse cut was made to remove the apex of the heart (**Fig. 1a**) and expose the left and right ventricles, then the atria and pulmonary artery were carefully removed proximal to the aortic root (**Fig. 1b**). The AV was then opened by cutting the commissure between the left and non-coronary (L-N) leaflets from the ventricular side and through the remaining mitral valve leaflet tissue (**Fig. 1c**). Each MAVL was resected by cutting at the aortic root base. MAVL tissues were carefully flattened onto the dopamine coated membrane surface by placing a leaflet in a ~3 µl 1xPBS droplet on the membrane and carefully aspirating the solution while simultaneously manipulating the leaflet until proper contact throughout the tissue surface was obtained (**Fig. 1d**).

Tissue Adhesion Verification

The Flexcell StageFlexer system could not be used to measure tissue-membrane adhesion since the maximum allowable strain (15%) did not induce tissue detachment. Therefore, tissue-membrane adhesion was tested by conducting uniaxial strain tests with an MTI SEMtester (Albany, NY, USA) on the composite to determine the strain

at which noticeable separation occurred. To assess the effect of dopamine concentration on tissue adhesion, two dopamine concentrations were tested, 0.1 and 0.5 mg/mL (n=1). After proper tissue adhesion, the surface of the membrane containing the MAVL is sprayed with red tissue marking dye while the other side is sprayed with blue acrylic paint. This aids in determining the time of interest (TOI), defined here as the point throughout the tensile test where noticeable detachment occurs evident by a difference in strain between the red and blue fiducial markers. Rectangular strips (15 x 7 mm) of the tissue-containing-membrane are cut out such that the leaflet resides near the center of the rectangular strip with the radial direction aligned parallel to the primary axis of strain (**Fig. 2a**). Uniaxial tension was applied and quantified using the MTI SEMtester (100 Hz sampling rate) while simultaneously recording the leaflet with a microscope video camera (30 frames per second) to determine the TOI. TOI was manually determined by scrubbing through video footage of the experiment and noting the grip to grip strain level at these time points.

MAVL Strain Testing

MAVLs were adhered near the center of the silicon rubber membrane coated with a 0.3 mg/mL dopamine solution ensuring proper adhesion and minimizing black dopamine precipitants at the higher 0.5 mg/mL concentration (n=6). Dopamine is an organic chemical that interacts with slightly basic pH solutions by a spontaneous oxidative reaction to form a layer of polydopamine, a type of melanin [14]. The silicone membrane was then loaded into a StageFlexer® Strain Device and 1xPBS was added to prevent drying (**Fig. 2b**). When a vacuum is applied, an equiaxial load is applied as the membrane deforms over a lubricated loading post [15]. Ten preconditioning cycles of 52.86 kPa load at 0.5 Hz were conducted prior to image acquisition. Microscopic images of the leaflet were acquired at five different vacuum pressures loads (6.72, 15.62, 26.44, 38.93, 52.86 kPa) using a FlexCell system (Flexcell FX-5000), resulting in five load-strain configurations. Each vacuum load was applied for 30 seconds, allowing for repositioning, refocusing, and preventing strain rate-dependent effects.

One image per load configuration of each MAVL sample was acquired using an upright microscope (Zeiss Axioscope Upright Fluorescent Microscope) with a monochromatic Axiocam attachment. ImageJ was used in conjunction with a "Bio-Formats" plug-in to display the microscope image data files. In the context of this report, radial and circumferential directions refer to the anatomy of aortic valve leaflets. These *in vivo* directions have unique mechanical properties that manifest as anisotropic leaflet behavior measured in biaxial testing. Therefore, we use the radial and

circumferential terminology on the resected leaflets to test this characteristic biaxial behavior as done previously for aortic valve leaflets from larger mammals. The circumferential leaflet direction within the acquired image coordinate system is manually determined and the radial direction is defaulted to be orthogonal to the circumferential direction (**Fig. 2c**). MAVL tissues have distinct melanocytic pigment patterns, which serve as trackable markers. Position of multiple markers at each configuration are recorded by using the "Multi-point" tool offered by ImageJ, which stores x and y coordinates of selected markers on the image. These markers are manually placed on distinct pigment patterns for consistency throughout configurations. A custom MATLAB script creates lines and calculates the angles and Euclidean distance between the permutations of all the markers at each configuration. Then, strain of each line at its corresponding load configuration is calculated as $\frac{\Delta L}{L_0}$, the engineering strain, with the 6.72 kPa load configuration serving as the original configuration (L_0) to ensure that the MAVL was under basal tension (i.e., not folded). Manual selection of the circumferential direction, with respect to the MAVL anatomical geometry (**Fig. 2c**), is used to determine the strains that fall within 10 degrees of the primary axes of the valve (radial and circumferential). Stiffness of the tissue-membrane composite is determined as the slope of a linear fit of the overall tissue strain-load curves.

Membrane Strain Verification

Verification of isotropic StageFlexer membrane displacement under the same load regimen as the tissue membrane composite was conducted by following the procedures outlined in the *Tissue Strain Testing* section with a single key difference. Tissue marking dye was sprayed on top of the membrane to serve as trackable fiducial markers on the otherwise transparent membrane surface.

Tissue Integrity and Fiber Alignment

To assess tissue viability, an assay for live/dead cell staining (LIVE/DEAD™ Viability/Cytotoxicity Kit) was performed after MAVL tissue mechanical testing. Images were obtained using the Zeiss fluorescent microscope (n=3). Images of calcein am and ethidium homodimer fluorescence can be seen in (**Fig. 3a**, green and red, respectively). To verify MAVL fiber structure after mechanical testing and confirm radially and circumferentially oriented elastin and collagen fibers respectively, two-photon emission fluorescence (TPEF) of elastin (red) and collagen (cyan) Second Harmonic Generation (SHG) were obtained (**Fig. 3b**). A home-built laser scanning non-linear microscope with a broadband femtosecond excitation laser (Element 600, Femtolasers, Austria) was used to obtain SHG images of

collagen and TPEF of elastin. Images were obtained by scanning a laser beam with a pair of galvanometer mirrors (Thorlabs, Newton, NJ, USA) and directing it into a 20×/1 NA water immersion objective (Olympus, Japan), via a dichroic mirror (655spxr, Chroma, Bellows Falls, VT, USA) to separate two-photon signals from a reflected fundamental wavelength. A pair of photo multiplying tubes (Hamamatsu, Japan) with bandpass filters (400 nm central wavelength/40 nm bandwidth and 480 nm central wavelength/40 nm bandwidth) recorded SHG and TPEF signals respectively. 1000 × 1000-pixel images were acquired at 0.5 frames per second, 10 images were averaged to improve the signal to noise ratio. In post-processing a smoothing filter was used with ImageJ (ImageJ, NIH, Bethesda, MD, USA, 2-pixel mean radius filter). Images were square rooted to improve visibility.

RESULTS

Tissue Adhesion Verification

MAVL tissues on the StageFlexer membranes remained attached throughout strain levels far beyond those capable by the FlexCell system (14.8%). The MTI SEMtester can reach strains of up to 200% with a starting axial length of 10 mm between the sample grips. Tissue placed on the 0.5 mg/mL dopamine coated membrane never showed signs of detachment while the tissue on the 0.1 mg/mL dopamine coated membrane showed signs of detachment at 172% strain (n=1) (**Table 1**).

Membrane Strain Verification

Directional strain was determined by binning measured lines between markers into 10-degree angle bins with respect to an arbitrary horizontal (**Fig. 4**). Similar to previous observations [15], an angle independence of the strain field on the isotropic lone silicone membrane indicate an equiaxial load field (**Fig. 4a**). However, an angle dependence is observed in the tissue-membrane composite, indicating anisotropic behavior (**Fig. 4b**).

MAVL Strain

Strain-load curves depict the mechanical properties of the tissue-membrane composite (**Fig. 5**) (n=6, biological replicates). Equiaxial tensile load on the tissue-membrane composite resulted in an orthotropic strain response (**Fig. 6**). Lone membrane radial stiffness using the same methodology mentioned earlier in this report was calculated to be

615 kPa (n=1). The tissue-membrane composite stiffness, calculated as the mean slope ± standard deviation of a linear fit for each curve, was 735 ± 162 kPa in the radial direction and 890 ± 153 kPa in the circumferential direction (**Fig. 6 a-c**). A paired T-test confirms a statistically significant difference (P=0.0006) between the radial and circumferential strains of these tissues (**Fig. 6d**). The mean difference between these orthogonal directions was 154.7 ± 8.8 kPa.

It is important to note that the term "stiffness" in the development of this method is used to describe the resistance to deformation by the tissue-membrane composite to the applied equiaxial load. This load is created by pulling a vacuum pressure within the StageFlexer chamber and is reported in kPa. Since engineering strain is a dimensionless measure of displacement, the slope of the linear fit to the load-displacement curves are in the units of kPa as well. This is not to be confused with the classical measure of stiffness from a standard stress-strain curve. Further development of this method would include a mathematical model to determine the applied stress and decouple the tissue characteristics from the tissue-membrane composite.

DISCUSSION

The present study developed a method in which MAVL biaxial tensile mechanics can be assessed by applying equiaxial tensile loads on a tissue-membrane composite while tracking the engineering strains on the surface of the tissue. Tensile biaxial mechanical properties of MAVL tissues have not been previously reported, thus this method may allow future studies to combine murine-based mechanistic studies of AV development and disease to MAVL mechanics. Similar to the characteristic orthotropic mechanical properties of human and porcine AVs, statistically significant orthotropic tissue level mechanics depict a stiffer circumferential direction compared to the radial direction. During lower load configurations the circumferential strains are higher than radial strains, whereas the radial strain becomes higher than the circumferential strain at higher loads, implicating possible collagen uncrimping of the tissues at intermediate strain levels. Previous studies have reported a similar response in porcine aortic valves, where crimped collagen fibers provide little resistance when small loads are applied but resist deformation once sufficient loads promote uncrimping of the collagen fibers [1].

The strain range provided by the FlexCell system (0-15%) limits the assessment of MAVL mechanics at high strains utilizing this method. It is possible that the biaxial response is more profound at higher levels of strain as seen with

larger mammal models. As with all soft tissues, MAVL tissues are expected to exhibit viscoelastic material properties. The non-linear displacement response to increasing load may be evident at higher strain values (>10%) as seen in larger mammal models testing the same tissues [16]. At the lower strains used in the current study (2-8%) the MAVL tissues exhibit a linear behavior. Further experimentation to determine the viscoelastic properties of MAVL tissues would necessitate more capable biaxial mechanical testing set ups as well as decoupling the leaflet behavior from the tissue-membrane composite. In future studies traditional biaxial tensile testers could be implemented using the tissue-membrane composite to assess the tissue response at higher levels of strain. Longer timescale experimentation using this method to controllably mechanically stimulate MAVL tissues would elucidate on the role of mechanical load on the various established mouse models of aortic valve disease.

Experiments were originally conducted with 8 leaflet samples; however, our analyses indicated that 2 of the samples did not remain attached throughout the duration of the mechanical testing regimen. The 2 poorly adhered samples were evident by either 1) visible tissue sections floating in solution (e.g., only the free edge would attach and the base would float), or 2) tension was observed in one direction and compression in another (Poisson's effect). If the materials are perfectly bonded, all directions would be in tension during the testing. The load-strain curves found by tracking surface markers are only applicable in measuring properties of the tissue-membrane composite if the tissue and membrane displace equally as a perfectly bonded composite material. Therefore, the poorly adhered leaflets were excluded from the study. For the 6 samples used in the study, perfect adhesion between the tissue and the membrane was assumed in the analyses. Further optimization needs to be performed to improve and verify proper adhesion prior to initiating mechanical testing.

Our results show variability in mechanical properties of MAVL tissues derived from different mice. Balani et.al. [8] report a difference in mechanical stiffness of MAVL tissues in areas of pigment compared to non-pigmented areas. Mouse aortic valves have asymmetric melanocytic pigment expression across the three leaflets, which could contribute to the observed variability between samples. We have consistently observed elevated pigmentation in the right and non-coronary MAVLs compared to the left coronary MAVL (**Fig. 1c**). In the current study, we did not track the MAVL (i.e., left coronary, right coronary, or non-coronary) used from each mouse for the tests. Future studies tracking

differences between the different MAVLs could yield insight into structural and mechanical differences within the aortic valve.

In addition to passive responses from extracellular matrix alignment, the tissue response to the applied tensile load may also be influenced by active cellular control of MAVL tonality. Dopamine is a common vasoconstriction stimulant used to treat various cardiovascular conditions such as low blood pressure and low heart rate and is synthesized in the synaptic space between neurons [17]. In the current study, we coat the membrane with dopamine followed by thorough washing prior to adding the tissue. Therefore, only endothelial cells should contact the dopamine coating and not the contractile cell populations that may control valve tone within the tissue. However, future studies would need to assess the effect of dopamine-coat on tissue biomechanics by using other adhesives and/or blocking dopamine receptors. Decoupling these responses in future studies will allow for a holistic understanding of the active and passive mechanical properties of WT mouse aortic valve tissues as well as those of genetically modified mice recapitulating aspects of human valve disease progression. Tissues seem to remain viable (**Fig. 3a**) with structurally intact extracellular matrix components (**Fig. 3b**) after resection and mechanical testing regimen. VIC contractility may influence the basal tonality of AV tissue [18]. A MAVL basal tone could be determined using this methodology in conjunction with the methods proposed by Chester et. al. [19] in which inhibition and activation of smooth muscle cell contractility uncovers the role these cell types play on AV tissue mechanics.

ACKNOWLEDGEMENT

The authors thank Kelsy Scott and Shreyanshu Ray for technical assistance, Drs. Jorge Riera, Alexander Agoulnik, and Lidia Kos for providing mouse tissues used in the study, and Dr. Nikolaos Tsoukias for providing access to equipment required for MAVL dissection.

.

FUNDING

Valentina Dargam was supported by a Ronald E. McNair Graduate Fellowship. A Scientist Development Grant from the American Heart Association supports Dr. Joshua D. Hutcheson (17SDG633670259).

REFERENCES

1. Sacks, M.S. and A.P. Yoganathan, *Heart valve function: a biomechanical perspective.* Philosophical transactions of the Royal Society of London. Series B, Biological sciences, 2007. **362**(1484): p. 1369-1391.
2. Tesfamariam, M.D., A.M. Mirza, D. Chaparro, A.Z. Ali, R. Montalvan, I. Saytashev, B.A. Gonzalez, A. Barreto, J. Ramella-Roman, J.D. Hutcheson, and S. Ramaswamy, *Elastin-Dependent Aortic Heart Valve Leaflet Curvature Changes During Cyclic Flexure.* Bioengineering (Basel), 2019. **6**(2).
3. Pham, T., F. Sulejmani, E. Shin, D. Wang, and W. Sun, *Quantification and comparison of the mechanical properties of four human cardiac valves.* Acta Biomater, 2017. **54**: p. 345-355.
4. Stella, J.A., J. Liao, and M.S. Sacks, *Time-dependent biaxial mechanical behavior of the aortic heart valve leaflet.* J Biomech, 2007. **40**(14): p. 3169-77.
5. Stella, J.A. and M.S. Sacks, *On the biaxial mechanical properties of the layers of the aortic valve leaflet.* J Biomech Eng, 2007. **129**(5): p. 757-66.
6. Sider, K.L., M.C. Blaser, and C.A. Simmons, *Animal models of calcific aortic valve disease.* Int J Inflam, 2011. **2011**: p. 364310.
7. Robert B. Hinton, J., C.M. Alfieri, S.A. Witt, B.J. Glascock, P.R. Khoury, D.W. Benson, and K.E. Yutzey, *Mouse heart valve structure and function: echocardiographic and morphometric analyses from the fetus through the aged adult.* American Journal of Physiology-Heart and Circulatory Physiology, 2008. **294**(6): p. H2480-H2488.
8. Balani, K., F. Brito, L. Kos, and A. Agarwal, *Melanocyte pigmentation stiffens murine cardiac tricuspid valve leaflet.* Journal of the Royal Society, Interface / the Royal Society, 2009. **6**: p. 1097-102.
9. Krishnamurthy, V.K., F. Guilak, D.A. Narmoneva, and R.B. Hinton, *Regional structure-function relationships in mouse aortic valve tissue.* J Biomech, 2011. **44**(1): p. 77-83.
10. Sewell-Loftin, M.K., C.B. Brown, H.S. Baldwin, and W.D. Merryman, *A novel technique for quantifying mouse heart valve leaflet stiffness with atomic force microscopy.* J Heart Valve Dis, 2012. **21**(4): p. 513-20.
11. Ayoub, S., G. Ferrari, R.C. Gorman, J.H. Gorman, F.J. Schoen, and M.S. Sacks, *Heart Valve Biomechanics and Underlying Mechanobiology.* Compr Physiol, 2016. **6**(4): p. 1743-1780.

12. Yang, K., J.S. Lee, J. Kim, Y.B. Lee, H. Shin, S.H. Um, J.B. Kim, K.I. Park, H. Lee, and S.W. Cho, *Polydopamine-mediated surface modification of scaffold materials for human neural stem cell engineering.* Biomaterials, 2012. **33**(29): p. 6952-64.

13. Poh, C.K., Z. Shi, T.Y. Lim, K.G. Neoh, and W. Wang, *The effect of VEGF functionalization of titanium on endothelial cells in vitro.* Biomaterials, 2010. **31**(7): p. 1578-85.

14. Lynge, M.E., R. van der Westen, A. Postma, and B. Stadler, *Polydopamine--a nature-inspired polymer coating for biomedical science.* Nanoscale, 2011. **3**(12): p. 4916-28.

15. Vande Geest, J.P., E.S. Di Martino, and D.A. Vorp, *An analysis of the complete strain field within FlexercellTM membranes.* Journal of Biomechanics, 2004. **37**(12): p. 1923-1928.

16. Anssari-Benam, A., D.L. Bader, and H.R. Screen, *A combined experimental and modelling approach to aortic valve viscoelasticity in tensile deformation.* J Mater Sci Mater Med, 2011. **22**(2): p. 253-62.

17. Swann, J.W., C.N. Sinback, M.G. Pierson, and D.O. Carpenter, *Dopamine produces muscle contractions and modulates motoneuron-induced contractions in Aplysia gill.* Cell Mol Neurobiol, 1982. **2**(4): p. 291-308.

18. Merryman, W.D., H.Y. Huang, F.J. Schoen, and M.S. Sacks, *The effects of cellular contraction on aortic valve leaflet flexural stiffness.* J Biomech, 2006. **39**(1): p. 88-96.

19. Chester, A.H., J.D. Kershaw, P. Sarathchandra, and M.H. Yacoub, *Localisation and function of nerves in the aortic root.* J Mol Cell Cardiol, 2008. **44**(6): p. 1045-52.

Table Caption List

Table 1 Uniaxial tensile tests were performed using an MTI SEMtester to identify adhesive properties of MAVL tissue to silicone rubber membrane using different dopamine concentrations. The strain at the time of detachment for both dopamine concentrations is greater than the applied strain in the experimental equiaxial mechanical testing regimen (10%)

Figure Caption List

Fig. 1 Preparation of MAVL on dopamine coated membrane. (a) Adult WT (C57/BL6) mouse heart. (b) Intact aortic root post-removal of surrounding tissues. (c) The valve is cut open at L-N coronary commissure to maintain leaflet integrity, thus exposing the leaflets. Cusps are resected by cutting close to the base of the leaflet. (d) The leaflet is then placed flat on a dopamine-coated StageFlexer® silicone rubber membrane.

Fig. 2 Experimental setup for uniaxial and equiaxial testing of tissue-membrane composite. (a) Tissue-membrane adhesion verification was tested by applying uniaxial tension to the sample, consisting of a rectangular strip of the membrane with the adhered leaflet, using an MTI SEMtester at room temperature with constant 1xPBS washes to prevent the tissue from drying. (b) StageFlexer dopamine coated membrane with sample, depicting the location of the leaflet on the loading station. (c) The leaflet circumferential and radial orientations were manually determined.

Fig. 3 MAVL tissue integrity and fiber alignment after mechanical stimulation. (a) Calcein AM (green) fluorescence and ethidium homodimer (red) fluorescence were used to image live and dead MAVL cells, respectively. (b) Two-photon microscopic images of circumferentially(c)-aligned collagen (SHG, cyan) and radially(r)-aligned elastin (TPEF, red) fibers.

Fig. 4 Mean measured strain experienced by the lone membrane and tissue-membrane composite. To measure strain, markers were manually selected and tracked on the membrane alone and tissue surface of the tissue-membrane composite for different applied vacuum pressure loads. The Euclidian distance between each marker was used to calculate the engineering strain. Strain was averaged and binned in 10 degree increments based on the arbitrary horizontal of the image. (a) Tissue marking dye speckle pattern markers on a silicone rubber membrane were used to verify the strain experienced by the isotropic membrane at each load configuration, indicating an equiaxial load field. (b) Pigment on a MAVL were used as trackable markers to measure the strain experienced by the tissue-membrane composite at each equiaxial load configuration. An angle dependent, anisotropic, behavior is observed.

Fig. 5 Strain-load curve for each MAVL tissue-membrane composite sample (dash line) and the mean of all samples (n=6, solid line). The stiffness for all samples, as defined by the slope of the mean strain-load curve, is 796 ± 157 kPa.

Fig. 6 Strain-load curve for each MAVL tissue-membrane composite sample (dash line) (n=6) and the mean of all samples (solid line), from orthogonal directions on the leaflet surface. (a) Circumferential strain-load curve. (b) Radial strain-load curve. (c) The tissue-membrane composite mean stiffness for all samples, as defined by the slope of the mean strain-load curve, is 735 ± 162 kPa in the radial direction (circles) and 890 ± 153 kPa in the circumferential direction (crosses). (d) Comparison of MAVL stiffness in the radial and circumferential strain directions are significantly different (paired t-test, two-tailed, 95% CI, $p<0.05$).

Journal of Biomechanical Engineering. Received January 02, 2020;
Accepted manuscript posted April 15, 2020. doi:10.1115/1.4046921

Table 1. **Tissue Adhesion Verification**	
Dopamine Concentration (mg/mL)	Strain at Detachment (%)
0.1	171.6
0.5	>200 (No evidence of detachment)

Journal of Biomechanical Engineering. Received January 02, 2020;
Accepted manuscript posted April 15, 2020. doi:10.1115/1.4046921

Figure 1

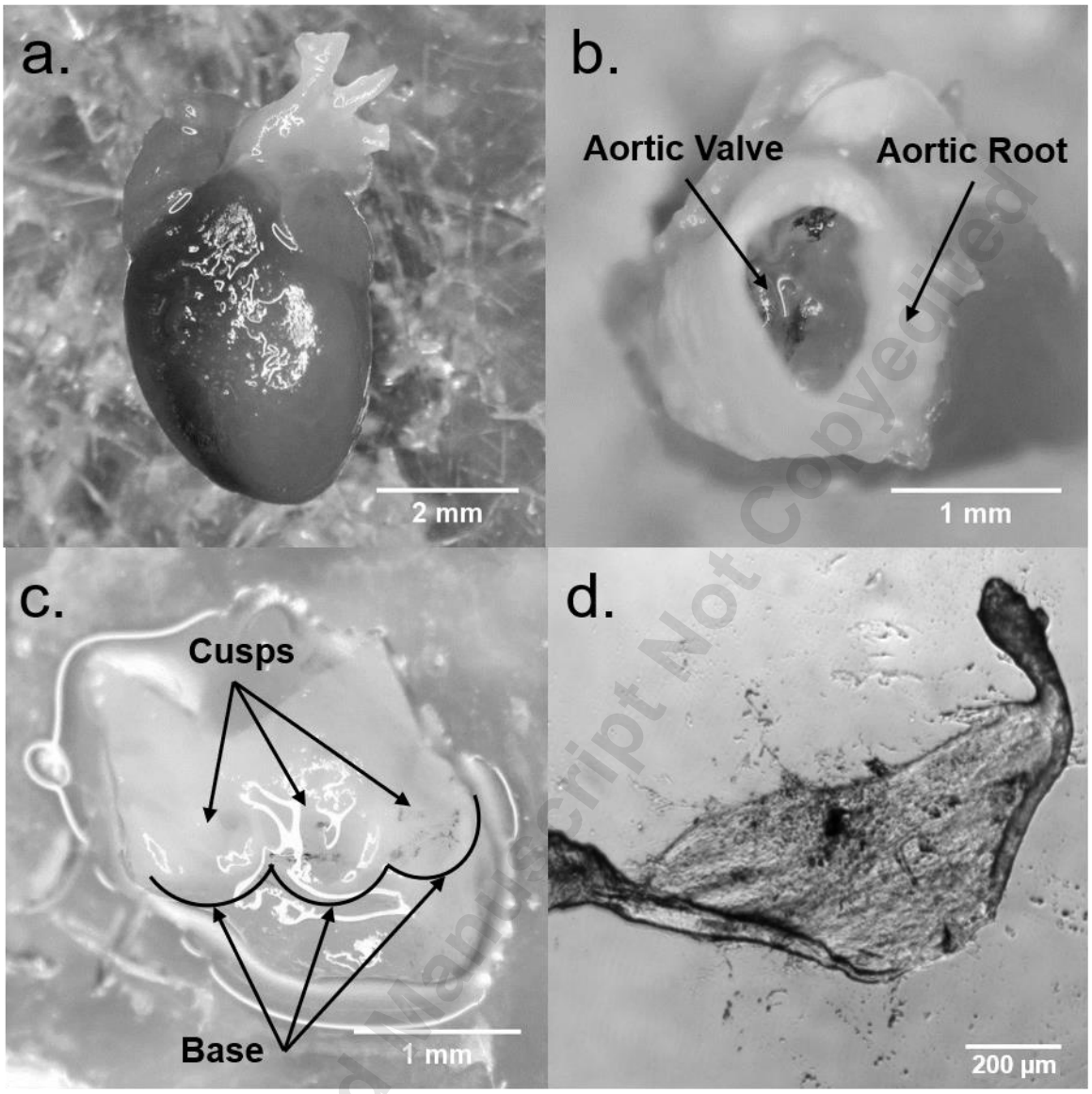

Journal of Biomechanical Engineering. Received January 02, 2020;
Accepted manuscript posted April 15, 2020. doi:10.1115/1.4046921

Figure 2

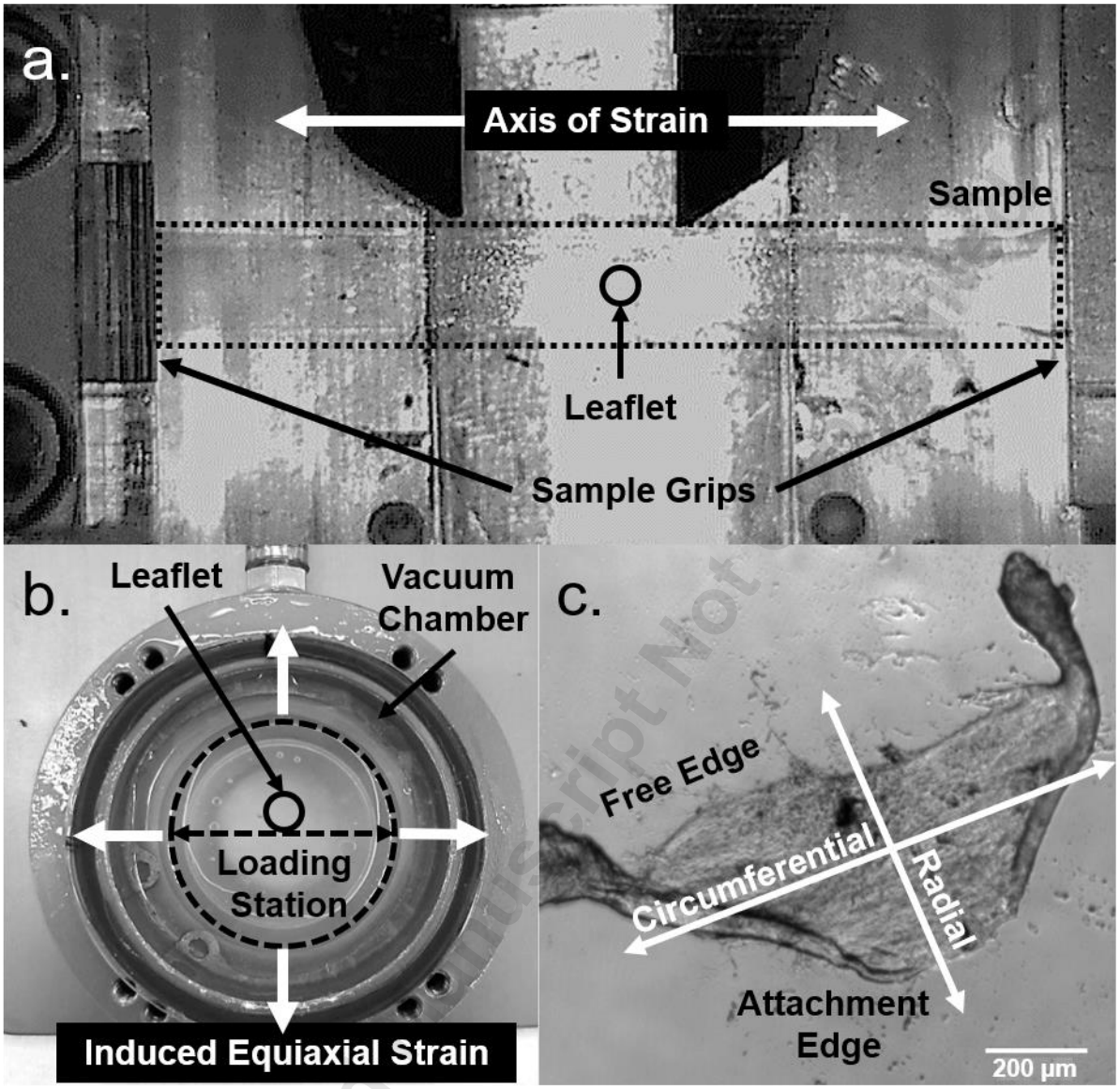

Journal of Biomechanical Engineering. Received January 02, 2020;
Accepted manuscript posted April 15, 2020. doi:10.1115/1.4046921

Figure 3

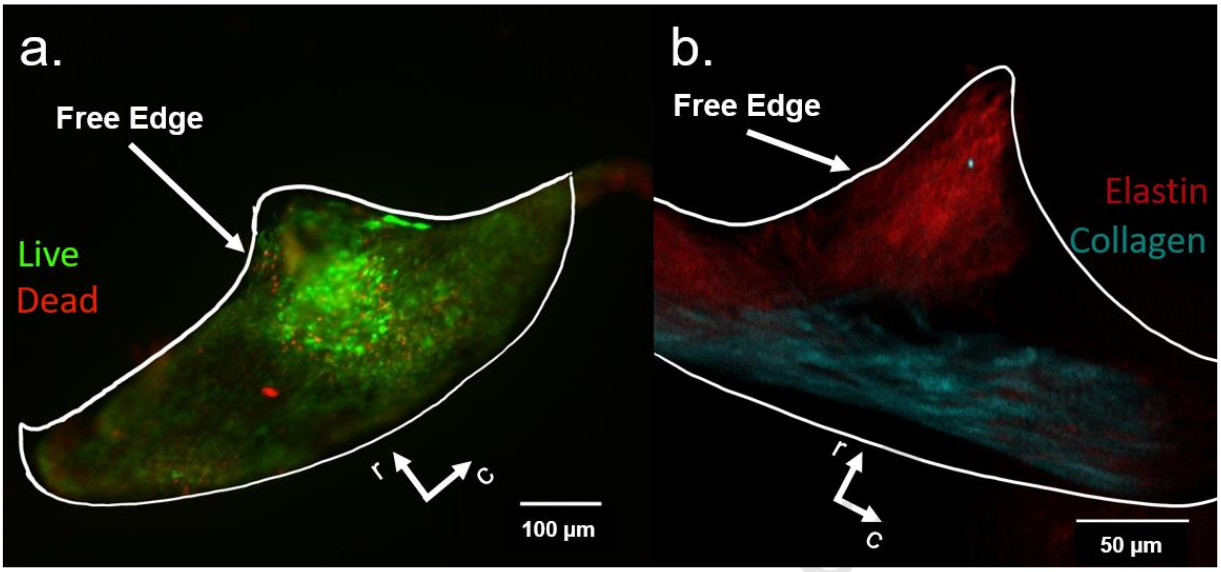

Journal of Biomechanical Engineering. Received January 02, 2020;
Accepted manuscript posted April 15, 2020. doi:10.1115/1.4046921

Figure 4

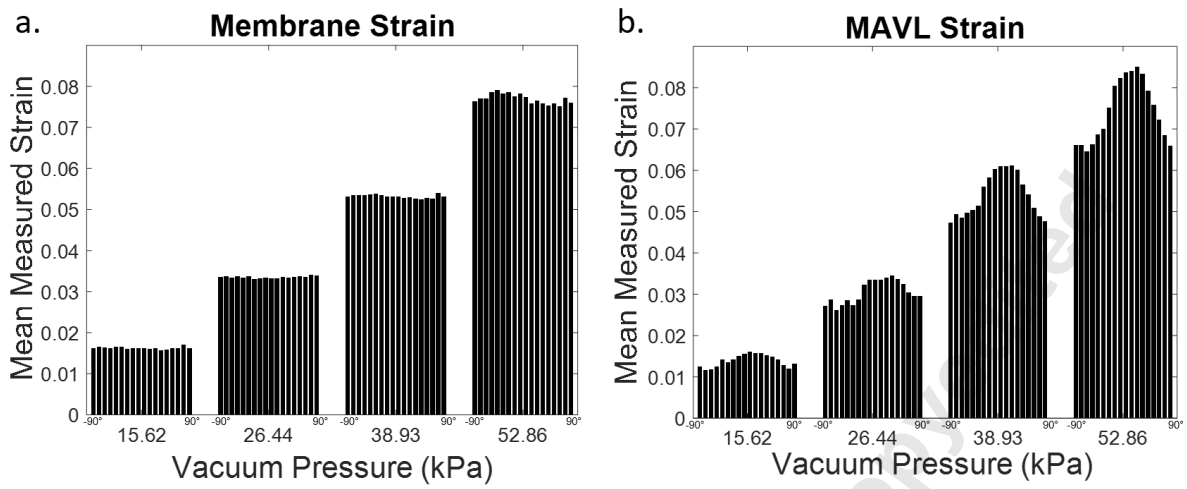

Journal of Biomechanical Engineering. Received January 02, 2020;
Accepted manuscript posted April 15, 2020. doi:10.1115/1.4046921

Figure 5

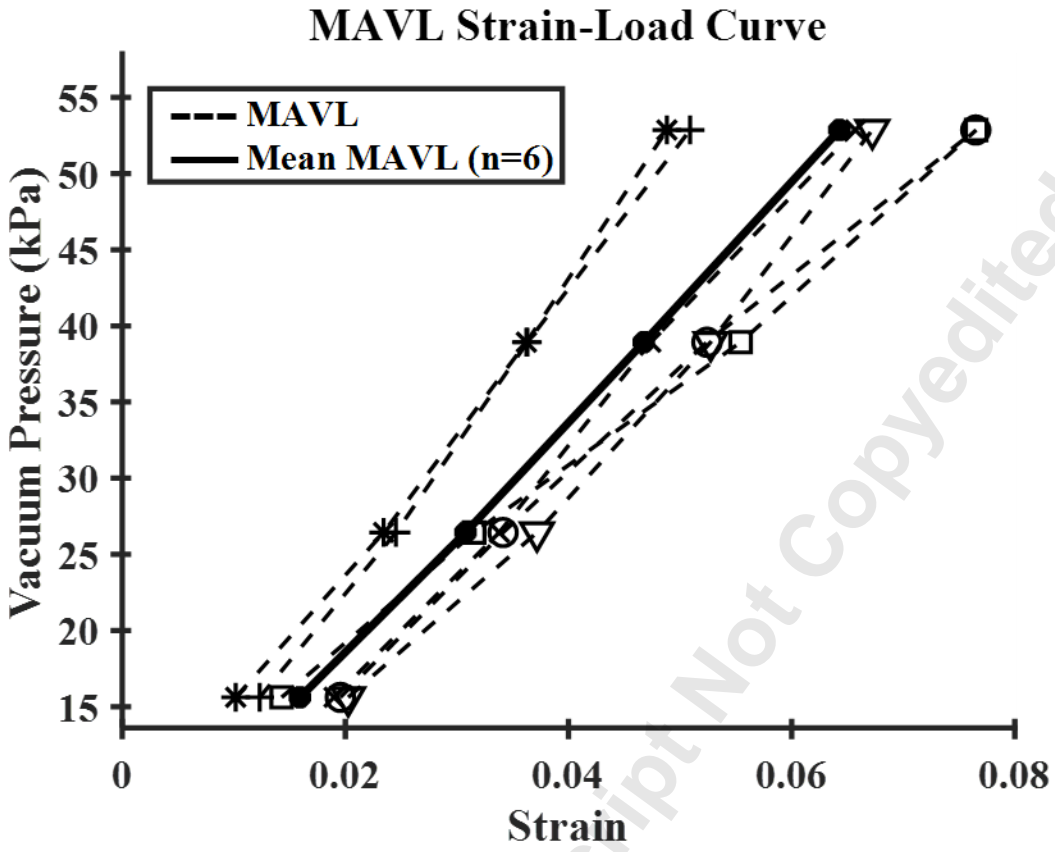

Journal of Biomechanical Engineering. Received January 02, 2020;
Accepted manuscript posted April 15, 2020. doi:10.1115/1.4046921

Figure 6